— | — Oak Ridge acc

Presented at the 13th Scintillation and Semiconductor Counter Symposium, 1-3 March 1972; will be published in the Proceedings either June or July 1972; tentative editor: Helen Cook

ACRH-1000-314
CONF-720306--5

Read at the 13th Scintillation and Semiconductor Counter Symposium, March 1-3, 1972, In Washington, D.C.

Sponsored Jointly by

I.E.E.E. Nuclear Science Group

U.S. Atomic Energy Commission

National Bureau of Standards

ASPECTS OF IMAGING AND COUNTING IN NUCLEAR MEDICINE USING SCINTILLATION AND SEMICONDUCTOR DETECTORS

by

R. N. Beck, L. T. Zimmer

D. B. Charleston, and P. B. Hoffer

Department of Radiology

University of Chicago and Argonne Cancer Research Hospital*

Chicago, Illinois

* Operated by the University of Chicago for the United States Atomic Energy Commission

DISCLAIMER

ASPECTS OF IMAGING AND COUNTING IN NUCLEAR MEDICINE USING SCINTILLATION AND SEMICONDUCTOR DETECTORS

by

R. N. Beck, L. T. Zimmer

D. B. Charleston, and P. B. Hoffer

Department of Radiology

University of Chicago and Argonne Cancer Research Hospital

Chicago, Illinois

SUMMARY

In the interest of minimizing patient irradiation, while maximizing diagnostic image quality, it is desirable to utilize all of the radiation emerging from the patient. For optimum utilization, it appears to be necessary to allow photons with different energies to contribute to the image with different weights. Optimum weights have been determined for the most common case of noise-limited images, where it is assumed that the weights should be chosen so as to maximize the signal-to-noise ratio. For less noisy images, sharpening may be achieved by assigning negative weights to scattered photons; that is, by scatter subtraction. In general, image formation with multiple weighted channels provides a greater degree of flexibility than is possible with a single channel.

INTRODUCTION

The principal goal of research on instrumentation in Nuclear Medicine is to improve the diagnostic quality of information derived from imaging procedures. These procedures include imaging of static and dynamic in vivo distributions of suitable stable and radioactive tracers. To minimize patient irradiation, while maximizing diagnostic image quality, it is necessary to make optimum use of the radiation emerging from the patient, a significant fraction of which consists of scattered photons due to Compton interactions within the patient. The question of how best to treat scattered radiation is a subject of considerable interest, since scatter affects both noise and contrast in the image. These effects can be quantified in terms of the effects of scatter on the sensitivity and spatial resolution of the imaging system. This paper summarizes the current status of our work on various aspects of the problem and suggests possible directions for the future.

PREVIOUS CONSIDERATIONS AND RESULTS

The object to be Imaged

If attention is confined to static radionuclide imaging, the object to be imaged can be thought of as a low-intensity, self-radiant, three-dimensional distribution of radioactive material embedded in a turbid medium which scatters and absorbs primary radiation emitted by the object. Thus, the radiation emerging from the patient consists of a line spectrum of unscattered photons and a continuous spectrum of photons scattered at all angles, which may be due to γ-rays emitted outside the detector field of view, as indicated on the right in Figure 1.

The Radiation Detector

Since the energy resolution of radiation detectors is imperfect, the pulse amplitude spectra due to scattered and unscattered photons overlap; thus, it is impossible to reject all pulses due to scattered photons by pulse height analysis without rejecting those due to primary radiation as well. A method for separating these components in the region of overlap has been developed[1] for analyzing spectra from large volume distributions. The result for ^{99m}Tc, using a NaI(Tl) scintillation detector, is shown in Figure 1, lower left.

The Scatter Fraction, f_s: Effect on Sensitivity and Dependence on E_s and θ

The separation of these spectra enables us to compute the scatter fraction*, f_s, which is defined as the fractional increase in response due to scattered photons over the response to properly collimated primary radiation. Thus, one effect of scatter is an increase in response (or apparent sensitivity of the detector) by the factor $(1 + f_s)$. This has the effect of reducing the relative magnitude of quantum noise in the image.

Clearly, the magnitude of the scatter fraction is a function of E_s, the base line setting of the single channel pulse height analyzer (SCA) [the upper discriminator is set just above the unscattered photopeak]. For a given primary photon energy, E_0, the expected value of the maximum scattering angle, θ, for accepted photons is determined by E_s from Compton's equation. As E_s is raised, the angle of acceptance is reduced. As a result, f_s and sensitivity are reduced, as shown in Figure 2, where f_s is plotted as a function of θ for four γ-ray energies, for spectra obtained from uniform volume distributions 16cm in diameter and 16cm high in H_2O, simulating the patient's head. Since f_s depends on the

---

* To conform with notation used in reference 2, the symbol f_s will be used here in place of S, which was used in references 1, 3, and 4.

probability that Compton scattering occurs within the patient, as well as the probability that the scattered photon will emerge to be detected, it is of interest to see that f_s is not radically different for primary radiation in the range from 140-510 keV, for values of E_B corresponding to the same angle of acceptance. We might, therefore, expect to observe approximately the same effects of scatter on image contrast and resolution for these radionuclides when the lower discriminator is set for the same angle of acceptance.

First Criterion

Since scattered photons may be due to primary radiation emitted at any point within the source, it is reasonable to assume as a first approximation that the scattered photons produce essentially the same effect as background, contribute more or less uniformly to all parts of the image, and reduce image contrast by the factor $1/(1 + f_s)$. In that case, the base line setting which minimizes the error in measuring the count rate due to unscattered photons, in the presence of a "background" due to scatter, may be regarded as the optimum setting. This error is given by

$$\epsilon = \sqrt{\frac{1 + f_s}{N_p \Psi}} \qquad (1)$$

where N_p is the total number of pulses due to primary photons within the photopeak, and Ψ is the fraction of these within the SCA window, Thus, Ψ and f_s are functions of E_B. On this assumption, the optimum base line settings for the sources considered in Figure 2 are given approximately by 0.9 times the primary γ-ray energy, E_0. For these settings, less than 5% of the pulses due to unscattered photons are rejected.[3] The dashed lines in Figure 2 indicate the scatter fractions and acceptance angles corresponding to these optimum settings. The associated scatter fractions differ by more than a factor of 2, and increase monotonically with decreasing γ-ray energy, with a value of f_s=0.38 for ^{99m}Tc.

For a given value of N_p the error ϵ can be further reduced only by reducing f_s and/or by increasing Ψ. This can be achieved by use of a detector with better energy resolution.

Use of a Large Ge(Li) Detector

Figure 3 shows the pulse amplitude spectra obtained from a brain phantom with ^{99m}Tc with a NaI(Tl) detector and a large

coaxial Ge(Li) detector, the latter having an area of approximately 14cm^2 and a length of approximately 6cm. The values of FWHM are 23 keV and 4 keV respectively for these detectors. Although the Ge(Li) detector is not a high resolution detector by the standards of research in physics it nevertheless permits the lower discriminator to be raised to 136 keV before any pulses due to unscattered photons are rejected. For this setting the angle of acceptance is 25°.

The effect of this on brain scans is shown in Figure 4. The image on the left was obtained with two NaI(Tl) detectors operated simultaneously to reduce scanning time. The image on the right was obtained with the Ge(Li) detector. The increase in image contrast over the brain lesion has been verified by sensitometric measurements on the film.

Although increased rejection of scatter clearly results in an improvement in image contrast, the principal problem with this Ge(Li) detector is reduced sensitivity; that is, we observe only about 1/3 as many counts as with a 2" diameter NaI(Tl) crystal, for which the collimator used in both scans was designed.

As a result of reduced sensitivity, the scanning time with the Ge(Li) detector is excessive, being approximately 45 minutes for one view of the head. Such a detector is not truly competitive with the standard 3" NaI(Tl) detectors commonly used. In fact, an almost identical result could be obtained (in terms of increased contrast and reduced sensitivity) by operating the scintillation detector with a base line setting of 146 keV, well above the optimum setting of 125 keV for this detector[4].

To some extent, this limitation will ultimately be overcome by 7.5cm diameter Ge(Li) detectors with a drifted depth greater than 1cm, and FWHM<4keV, which are believed to be feasible.

Meanwhile, we have pursued the question of how best to utilize information from Ge(Li) detectors.

Second Criterion

The assumption that scatter is like background is reasonably valid for low energy γ-rays, using a scintillation detector, where the angle of acceptance corresponding to the optimum base line setting is large. However, this assumption

is less valid for high energy γ-rays, using a NaI(Tl) detector, and for low energy γ-rays using a Ge(Li) detector, since only photons scattered through small angles are accepted. In these cases, image contrast is less degraded by scatter, since photons scattered through small angles tend to resolve object structures.

In situations where scattered radiation tends to resolve object structures of interest, a more general and appropriate criterion for optimizing the base line setting is the Figure of Merit

$$Q = \frac{(C_T - C_0)^2}{(C_T + C_0)} \qquad (2)$$

where C_T is the count rate over a suspected tumor and C_0 is the count rate over normal tissue. Maximizing this quantity is equivalent to maximizing the signal-to-noise ratio that can be achieved per unit of observation time to distinguish between C_T and C_0.

Although some limited use has been made of this criterion to optimize E_B for scintillation detectors[4,5,6], it serves here as the basis for a more general formulation, discussed under Fourth Criterion, below.

AN EXTENSION AND GENERALIZATION

Scatter Subtraction

Heretofore we have considered only the possibilities of accepting or rejecting pulses due to scattered photons. An analysis by Zimmer suggests that subtraction of scatter may provide an attractive alternative, since this would produce a sharpened image. This alternative has been explored superficially in the following experiment.

Figure 5 shows two SCA windows set on a ^{99m}Tc spectrum obtained with the Ge(Li) detector. The upper window brackets the primary peak while the lower window accepts pulses due to photons scattered through angles between 25° and 55°.

Figure 6 shows the response of this system to a line source of ^{99m}Tc in a scattering medium, while Figure 7 shows the result of adding and subtracting these response functions. Addition yields a response function similar to

that ordinarily obtained with a scintillation detector and a single window, while subtraction yields a bipolar function with a positive central region and negative side lobes. The latter is the typical shape of a filter function that produces a sharpening effect.

Figure 8 shows the expected images of a step source, obtained by convoluting these response functions with a unit step function. The images have been normalized to show the effect of the response functions on the shape of the image. The least sharp image was obtained with the scatter channel alone, while the sharpest image was obtained by subtracting the scatter channel from the peak channel.

This result is consistent with what might be expected from a comparison of the modulation transfer functions (MTF) associated with these response functions, as shown in Figure 9. Since the MTF(ν) is a measure of the efficiency with which modulation of object sinusoids is transfered to the image, an ideal imaging system would have an MTF(ν)=1 for all spatial frequency components in the object. In Figure 9, the transfer function associated with scatter subtraction rises slightly above 1 in the low frequency range and is uniformly highest at all spatial frequencies.

The overshoot observed with scatter subtraction in Figure 8, and values of MTF>1 in Figure 9, indicate that too much scatter has been subtracted in this instance. That is, if less scatter were subtracted, or if less weight were given to pulses in the scatter channel, then we might obtain an image without overshoot, which would look more like the object, except for the residual unsharpness due essentially to the collimator alone. This fact suggests a more general formulation of the problem of how best to treat scatter.

Continuous Weights

In the preceding discussion we have considered the consequences of accepting, rejecting, and subtracting scattered radiation in the image forming process. These alternatives can be described as a choice between weighting factors of +1, 0, and -1 for scattered photons.

Clearly, this does not exhaust the possibilities, since we can easily conceive of imaging processes in which any finite positive or negative weight is given to each detected photon, In any particular case the weight might be a function of the photon energy, the absolute or relative number of photons at each energy, position or time, etc., or any combination of such parameters.

Optimum Weights

In general, if we conceive of the situation as one in which a human observer-analyst is called upon to extract diagnostic information from images, then each detected photon should be given a weight that depends upon the degree to which photons in its class (however defined) contribute to the formation of an image in which structures relevant to an accurate diagnosis will be detected by the observer-analyst with greatest probability.

In particular, if attention is confined to photon energy as a parameter, and if the entire pulse amplitude spectrum is divided into k discrete channels with width ΔE, and a fixed weight w_j (j=1, 2, ..., k) is given to pulses in each channel, the question that arises is: "What is the optimum weight for each channel?"

In general, the answer to this question depends upon the criterion adopted, which in turn depends upon a variety of factors concerning the objects to be imaged, the imaging system, and the observation time. Only two special cases will be discussed briefly.

Third Criterion (For the "noise-free" image)

If the number of photons recorded per unit area in the image is so large that the signal-to-noise ratio is high even for the smallest structures of interest, then weighting factors may be chosen to maximize the correspondence between the object and image. Linfoot[7] has discussed several measures of correspondence that may be useful. This will in general require sharpening the image to compensate for imperfect spatial resolution of the collimated detector. In general, all such sharpening procedures reduce the signal-to-noise ratio, and image sharpening by scatter subtraction is no exception; however, there appears to be no a priori reason to believe that this method would be more costly of signal-to-noise ratio than existing methods.

Fourth Criterion (For the "noise-limited" image)

The most common situation is also the most difficult; namely, when the signal-to-noise ratio (SNR) is so low that every effort must be made to raise the signal above the threshold of detectability.

If we wish to maximize the signal-to-noise ratio for a particular spatial frequency component, ν cycles/cm, it is shown in Appendix B [equation A(12)] that the weight

which should be given to pulses in the j^{th} channel is simply proportional to the value of the Detector Transfer Function* $S_j(\nu)$ at the frequency ν, for that channel. For the particular case discussed above, the optimum weights for the Peak and Scatter channels can be read from the respective MTF(ν) graphs in Figure 9.

In addition, if we wish to maximize the SNR for detecting an arbitrary object structure, it is shown in Appendix C that the optimum weight for each channel is simply proportional to the image contrast provided by the channel. The resulting maximum rate at which $[SNR]^2$ can be achieved is equal to the sum of Figure of Merit values for all channels. [See equation A(19)]

DISCUSSION AND CONCLUSIONS

Implementation of Variable Weights

The theory of variable weights provides an extremely general basis on which to develop a theory of optimum utilization of all radiation that emerges from the patient.

In the absence of precise knowledge about the values of weighting factors w(E) that would maximize the probability of an accurate diagnosis, the most conservative approach would be to record the amplitude, as well as the position coordinates, of each detected photon for subsequent off-line synthesis and examination of multiple images, based on different assumptions concerning optimum weights. These assumptions might include the entire range of weights between the extremes implied by the criteria for the noise-free and noise-limited images described above.

If stable optimum weights should be found for routine, standardized, imaging procedures, then it might be desirable to implement these weights on-line, to eliminate further image processing. Although any number of techniques can be imagined to accomplish this end, the design of a practical system may provide a stimulating challenge.

In view of the superior energy resolution of Ge(Li) and Si(Li) semiconductor detectors over NaI(Tl) scintillation

---

* This function is the Fourier Transform of the detector spread function, and has heretofore been called the Modulation Transfer Function in Nuclear Medicine[1-6]. To conform with nomenclature in Optics and Radiology, it is suggested[8] that the latter term be used only to refer to the absolute value of $S(\nu)$; that is, $MTF(\nu) \equiv |S(\nu)|$. When $S(\nu)$ is real and positive $MTF(\nu) = S(\nu)$.

detectors, any such variable weighting procedure might best be accomplished with a semiconductor detector. However, the sensitivity of semiconductor detectors must be increased before they become truly competitive with scintillation detectors.

ACKNOWLEDGEMENT

The authors are extremely grateful to Dr. Charles E. Metz for providing insight into alternative interpretations of the theory of optimum weights, and to Nuclear Diodes Inc. for providing the $Ge(Li)$ detector.

REFERENCES

1.) Beck, R.N.: A theory of radioisotope imaging systems, Medical Radioisotope Scanning, IAEA, Vienna, 1964, Vol. 1, pp. 35-56.

2.) MacIntyre, W.J., Fedoruk, S.O., Harris, C.C., Kuhl, D.E., and Mallard, J.R.: Sensitivity and Resolution in Radioisotope Scanning. Medical Radioisotope Scintigraphy, IAEA, Vienna, 1969, Vol. 1, pp. 391-435.

3.) Beck, R.N., Schuh, M.W., Cohen, T.D., Lembares, N.: Effects of Scattered Radiation on Scintillation Detector Response. Medical Radioisotope Scintigraphy, IAEA, Vienna, 1969, Vol. 1, pp. 595-616.

4.) Beck, R.N., Zimmer, L.T., Charleston, D.B., Hoffer, P.B., and Lembares, N.: The Theoretical Advantages of Eliminating Scatter in Imaging Systems. Semiconductor Detectors in Nuclear Medicine, pp. 92-113, (Hoffer, P.B., Beck, R.N., and Gottschalk, A. editors). Society of Nuclear Medicine, Publisher, New York, (1971).

5.) Beck, R.N., and Harper, P.V.: Criteria for Comparing Radioisotope Imaging Systems. Fundamental Problems in Scanning, pp. 348-384, (A. Gottschalk and R.N. Beck, editors). Charles C. Thomas, Springfield, Illinois, (1968).

6.) Sanders, T.P., Sanders, T.D., and Kuhl, D.E.: Optimizing the Window of an Anger Camera for ^{99m}Tc. J. Nuc. Med., 12 (11), p. 703, (1971).

7.) Linfoot, E.H.: Optical Image Evaluation, Focal Press, New York, (1964).

8.) Beck, R.N.: Nomenclature for Fourier Transforms of Spread Functions of Imaging Systems Used in Nuclear Medicine, J. Nuc. Med., (In Press).

APPENDICES

A. The Detector Transfer Function, $S_D(\nu)$

Assume that the energy range of the pulse amplitude spectrum is divided into k channels with width ΔE. Let $L(x;E_j) \equiv L_j(x)$ be the line source response function for the j^{th} channel, and let

$$n_j = \int_{-\infty}^{\infty} L_j(x)\,dx \qquad A(1)$$

be the number of counts expected to occur in this channel per unit observation time. If w_j is the weight given to each of these counts, the overall weighted line source response function is given by

$$L(x) = \sum_{j=1}^{K} w_j L_j(x) = \sum_{j=1}^{K} w_j n_j \ell_j(x) \qquad A(2)$$

where $\ell_j(x)$ is the line spread function, and

$$\int_{-\infty}^{\infty} \ell_j(x)\,dx = 1 \text{ for all } j. \qquad A(3)$$

With $\sum$ designating $\sum_{j=1}^{K}$, the Detector Transfer Function $S_D(\nu)$ is defined by

$$S_D(\nu) \equiv \frac{F.T.[L(x)]}{\int_{-\infty}^{\infty} L(x)\,dx} = \frac{\sum w_j n_j S_j(\nu)}{\sum w_j n_j} \qquad A(4)$$

where the Detector Transfer Function for the j^{th} channel is

$$S_j(\nu) \equiv F.T.[\ell_j(x)] = \int_{-\infty}^{\infty} \ell_j(x) e^{-2\pi i \nu x}\,dx$$

$$= \frac{\int_{-\infty}^{\infty} L_j(x) e^{-2\pi i \nu x}\,dx}{\int_{-\infty}^{\infty} L_j(x)\,dx} \qquad A(5)$$

In this nomenclature [8] the overall Modulation Transfer Function for the detector is defined by

$$MTF_D(\nu) \equiv |S_D(\nu)| \qquad A(6)$$

and for the j^{th} channel, by

$$MTF_j(\nu) \equiv |S_j(\nu)| \qquad A(7)$$

B. Optimum Weighting Factors for Detection of an Object Sinusoid

Let $N_j(x)\left[\frac{\text{counts}}{\text{cm}^2}\right]$ define the image of an object sinusoid with modulation $m_0(\nu)$, mean intensity $\bar{\sigma}\left[\frac{\text{photons}}{\text{cm}^2\text{-sec}}\right]$, and spatial frequency ν [cycles/cm], formed by the j^{th} channel; thus,

$$N_j(x) = \bar{N}_j + \tilde{N}_j(\nu)\cos 2\pi\nu x \qquad A(8)$$

The image modulation is given by

$$m_{ij}(\nu) \equiv \frac{\tilde{N}_j(\nu)}{\bar{N}_j} = m_0(\nu)S_j(\nu) \qquad A(9)$$

If the signal associated with this sinusoid is regarded as the difference in the expected numbers of counts under positive and negative half-cycles, then the signal for the j^{th} channel, is proportional to $\tilde{N}_j(\nu)$.

Similarly, if the noise associated with this sinusoid is regarded as the random fluctuation in the signal, measured by the standard deviation of the signal, then the noise associated with the j^{th} channel is proportional to $\sqrt{\bar{N}_j}$.

If each count in the j^{th} channel contributes to the image with weight w_j, the total weighted signal for all channels is proportional to $\sum w_j\tilde{N}_j(\nu)$, the total weighted noise is proportional to $\sqrt{\sum w_j^2\bar{N}_j}$, and the [Signal-to-Noise ratio]^2 is given by

$$[SNR]^2 \propto \frac{\left[\sum w_j\tilde{N}_j(\nu)\right]^2}{\sum w_j^2\bar{N}_j} \qquad A(10)$$

The optimum weight, w_j, which maximizes SNR, is found by solving $\frac{d[SNR]^2}{dw_j} = 0$ for w_j. Using equation (9), this procedure yields

$$w_j = S_j(\nu) \frac{\sum w_j^2 \bar{N}_j}{\sum w_j S_j(\nu) \bar{N}_j} \qquad A(11)$$

which is satisfied when

$$w_j(\text{opt}) = S_j(\nu) \qquad A(12)$$

With optimum weights, and using equation (9), the maximum value of $(SNR)^2$ is

$$[SNR]^2_{MAX}(\nu) \propto m_0^2(\nu) \sum \bar{N}_j S_j^2(\nu)$$
$$= \bar{\sigma} m_0^2(\nu) \sum_{j=1}^{K} \bar{S}_j \cdot S_j^2(\nu) \qquad A(13)$$

where

$$\bar{S}_j \equiv \frac{\bar{N}_j}{\bar{\sigma}} \qquad A(14)$$

is the sensitivity of the j^{th} channel to a uniform plane distribution.

Similarly, the Detector Transfer Function with optimum weights is found by substituting equation (12) in equation (4), and recognizing that $n_j \propto \bar{S}_j$,

$$S_D(\nu)\text{opt} = \frac{\sum n_j S_j^2(\nu)}{\sum n_j S_j(\nu)} = \frac{\sum \bar{S}_j \cdot S_j^2(\nu)}{\sum \bar{S}_j \cdot S_j(\nu)} \qquad A(15)$$

Equation (13) is a generalization of the result obtained previously for a single channel.[3]

C. Optimum Weighting Factors for Detection of Arbitrary Objects

Let N_{tj} and N_{oj} be the expected numbers of counts in the j^{th} channel associated with a suspected tumor region, and a normal region of the same size, respectively. Let $(N_{tj} - N_{oj})$ be the signal associated with this channel and let the standard deviation about the signal, $\sqrt{N_{tj} + N_{oj}}$, be a measure of the noise.

The total weighted signal and noise for all channels are given by $\sum w_j(N_{tj} - N_{oj})$ and $\sqrt{\sum w_j^2(N_{tj} + N_{oj})}$, respectively. The [signal-to-noise ratio]^2 is given by

$$[SNR]^2 = \frac{\left[\sum w_j(N_{tj} - N_{oj})\right]^2}{\sum w_j^2(N_{tj} + N_{oj})} \qquad A(16)$$

Solving $\frac{d[SNR]^2}{dw_j} = 0$ for w_j yields the optimum weight,

$$w_j(opt) = \frac{(N_{tj} - N_{oj})}{(N_{tj} + N_{oj})} \qquad A(17)$$

which can be interpreted as a measure of the contrast provided by the j^{th} channel.

Using optimum weights,

$$[SNR]^2_{MAX} = \sum_j \frac{(N_{tj} - N_{oj})^2}{(N_{tj} + N_{oj})} \qquad A(18)$$

If t sec is the observation time for each of these regions, which produce mean count rates C_{tj} and C_{oj} respectively, then the maximum rate at which $[SNR]^2$ can be achieved is given by

$$Q_{MAX} = \frac{[SNR]^2_{MAX}}{t} = \sum_j^K \frac{(C_{tj} - C_{oj})^2}{(C_{tj} + C_{oj})} = \sum_j^K Q_j \qquad A(19)$$

The sum of Figure of Merit values for all channels is greater than Q in equation (2) for one SCA which optimally brackets the photopeak, or which includes the entire spectrum.

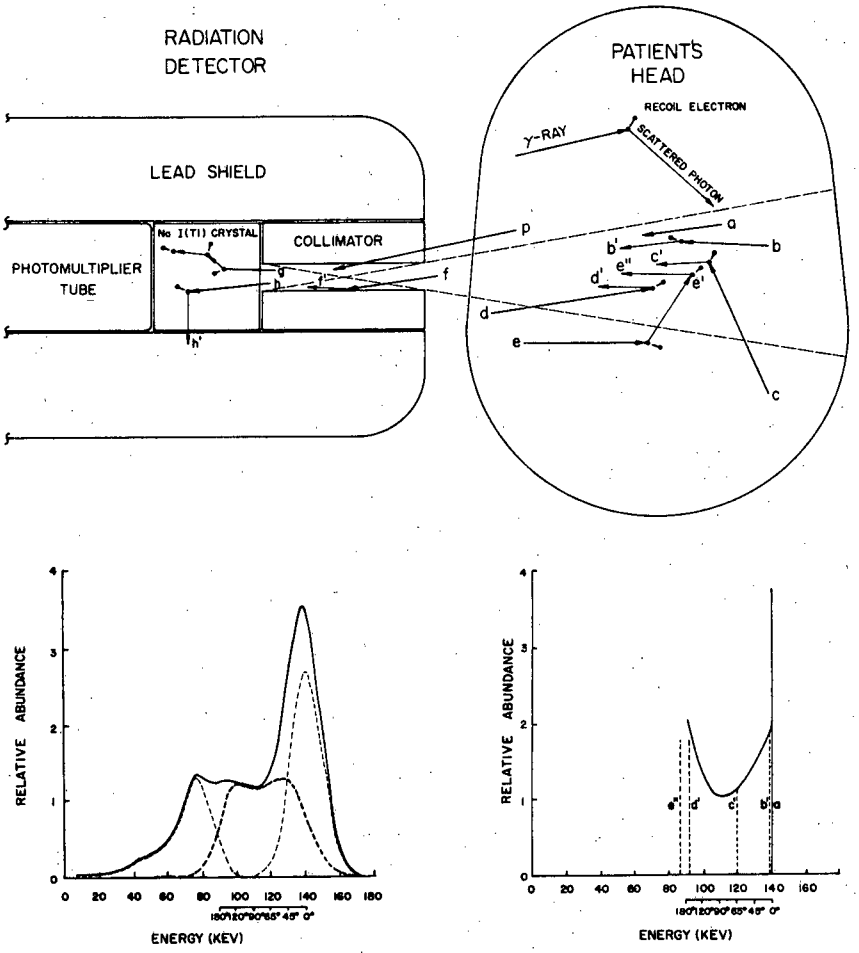

Figure 1. In brain scanning with ^{99M}Tc and a NaI(Tl) detector, the output pulse amplitude spectra due to scattered and unscattered photons overlap appreciably because of imperfect energy resolution of the detector.

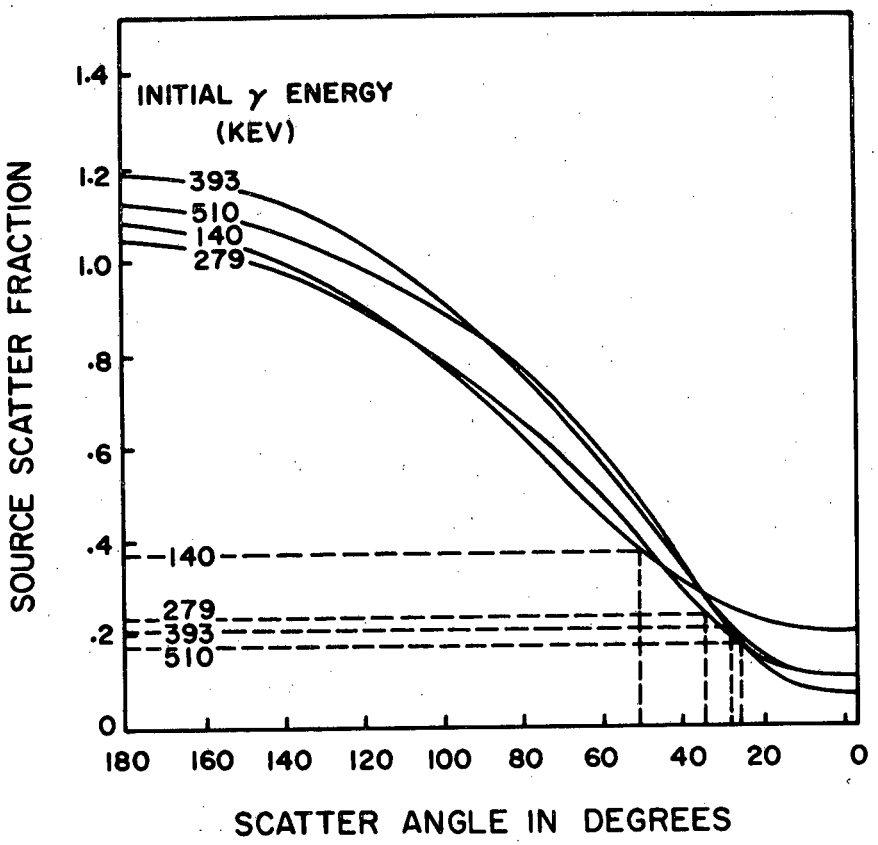

Figure 2. When the scatter fraction f_s is plotted as a function of the photon scattering angle corresponding to the base line setting, values of f_s are similar for all isotopes considered. The dashed lines indicate the "optimum" settings, assuming scatter is like background.

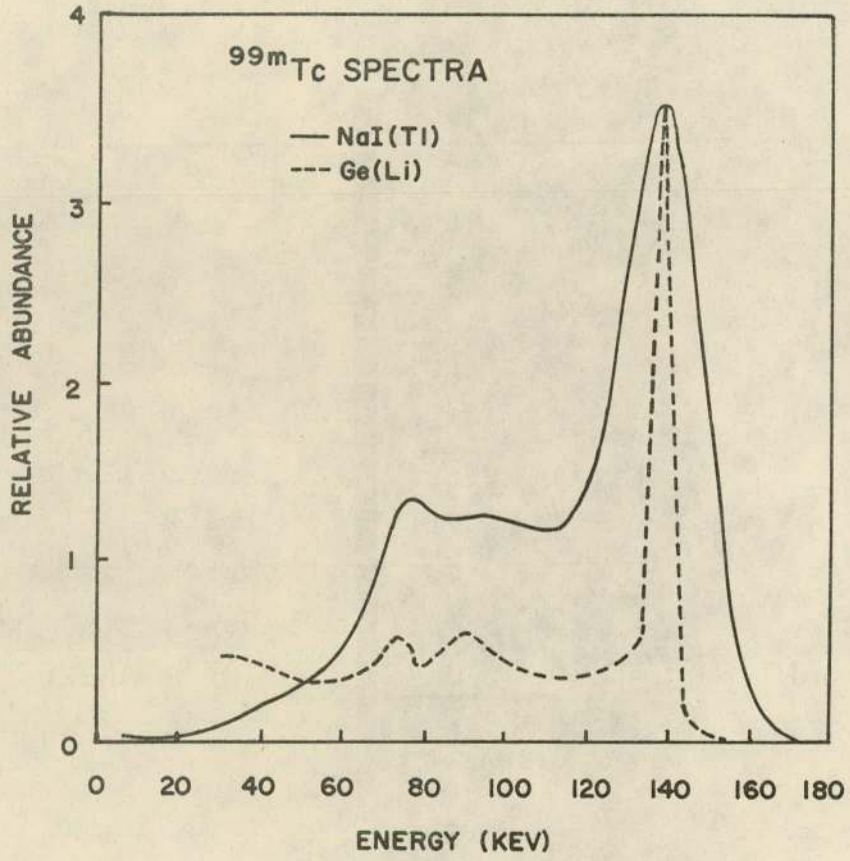

Figure 3. Improved energy resolution obtainable with a Ge(Li) detector permits rejection of all but small-angle scatter. The angle of acceptance is 55° for E_β = 125 keV and 25° for E_β = 136 keV.

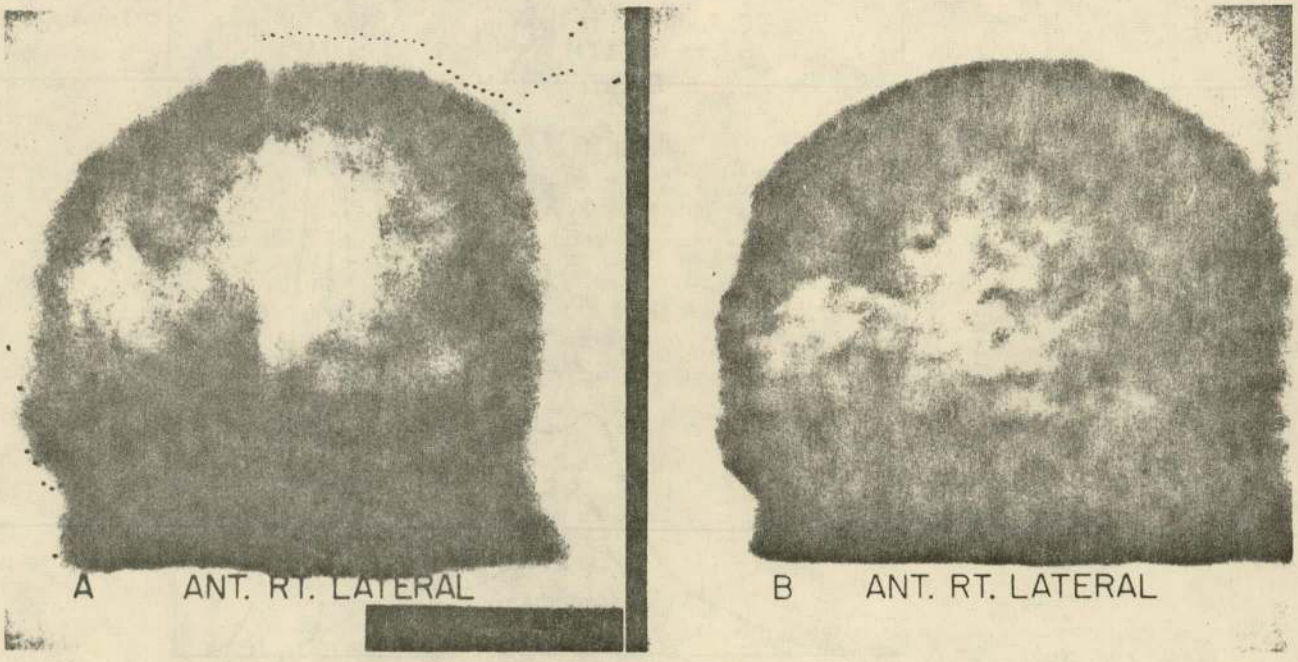

Figure 4. Lateral brain scans of the same patient with NaI(Tl) detectors (left) and a Ge(Li) detector (right). Note increased image contrast and improved perceptibility of the lesion.

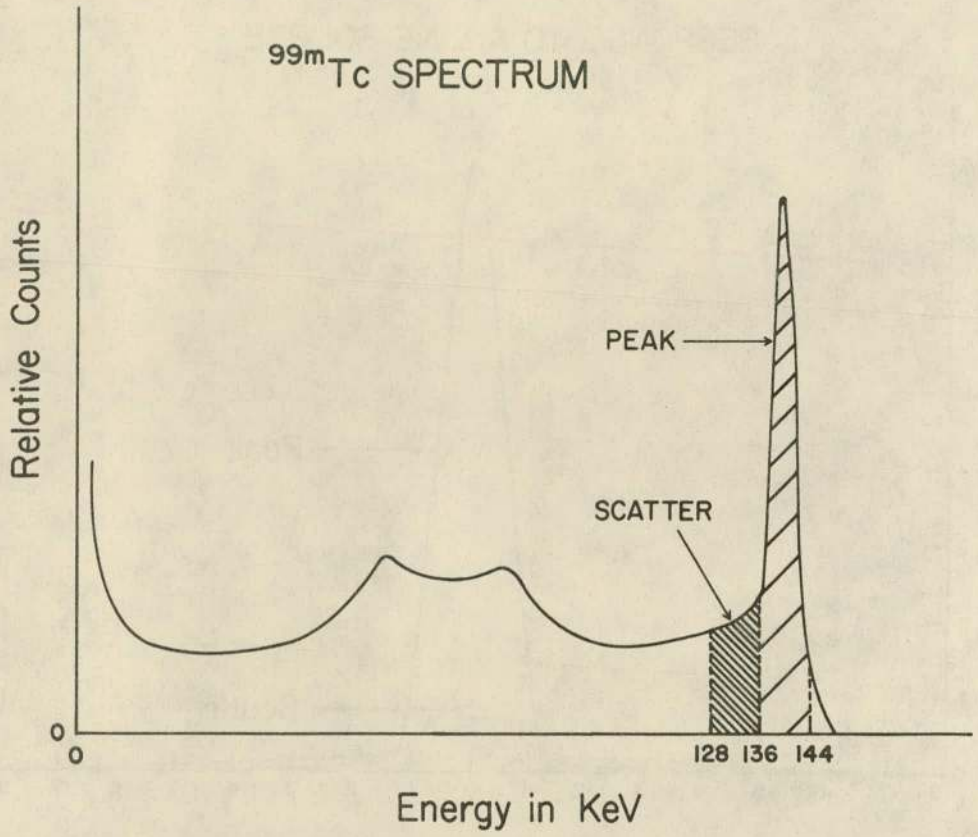

Figure 5. The peak due to unscattered photons is bracketed by one SCA while another covers the range of photons scattered through angles between 25° and 55°.

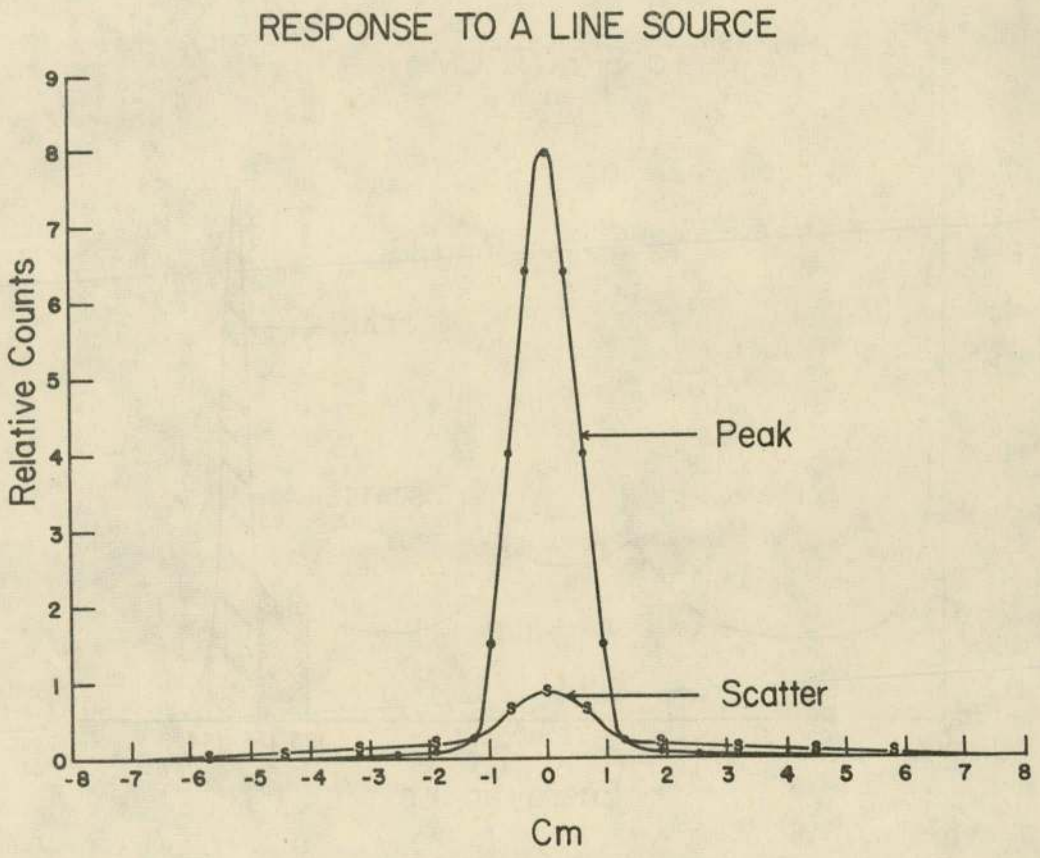

Figure 6. Line source response functions for the SCA windows shown in Figure 5. Note long tails due to Compton scattering within the source.

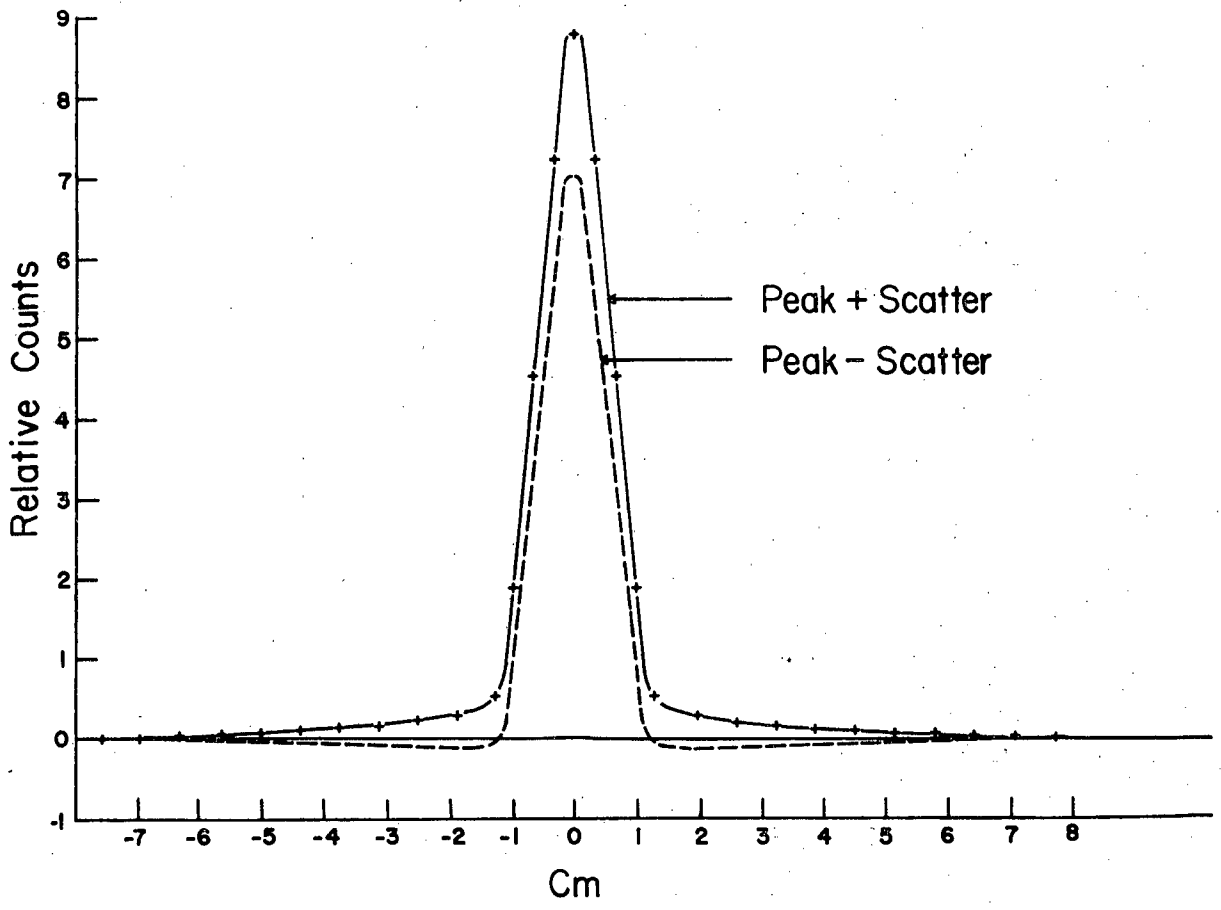

Figure 7. The sum and difference of response functions in Figure 6. Note bipolar nature of Peak-Scatter.

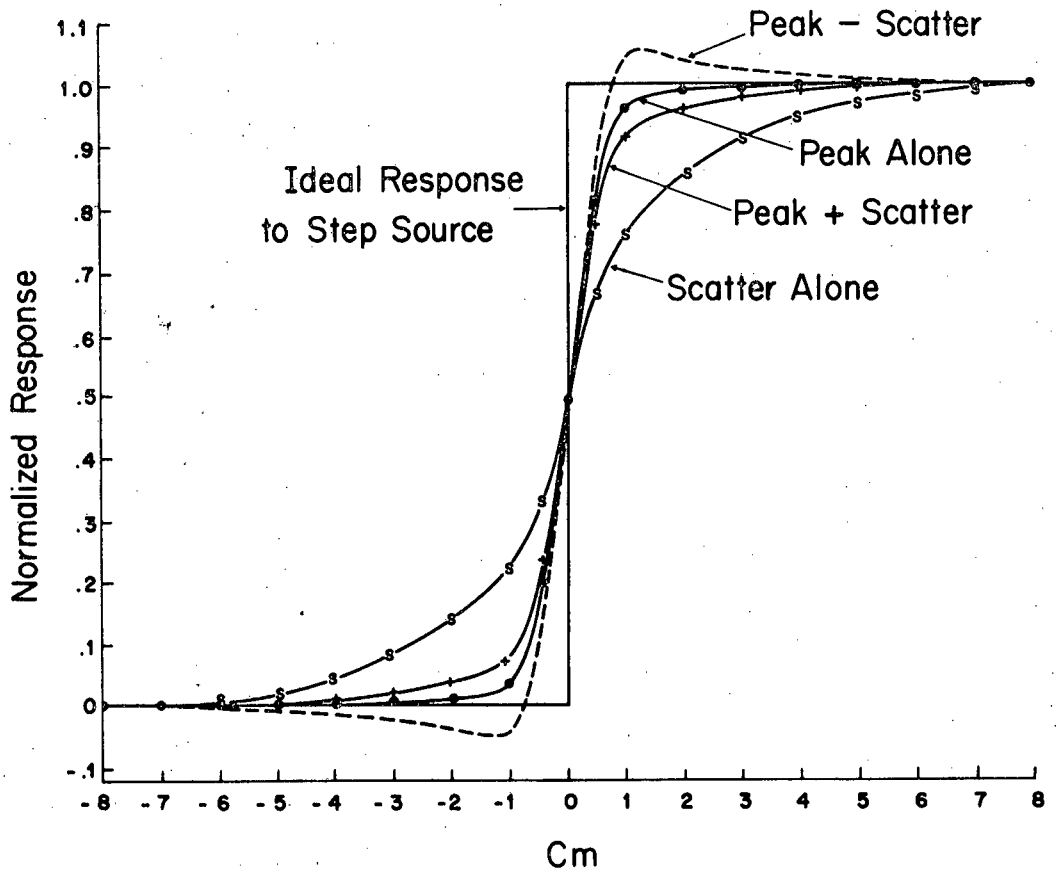

Figure 8. Expected images of a unit-step obtained with response functions in Figures 6 and 7. Note that scatter subtraction yields sharpest image.

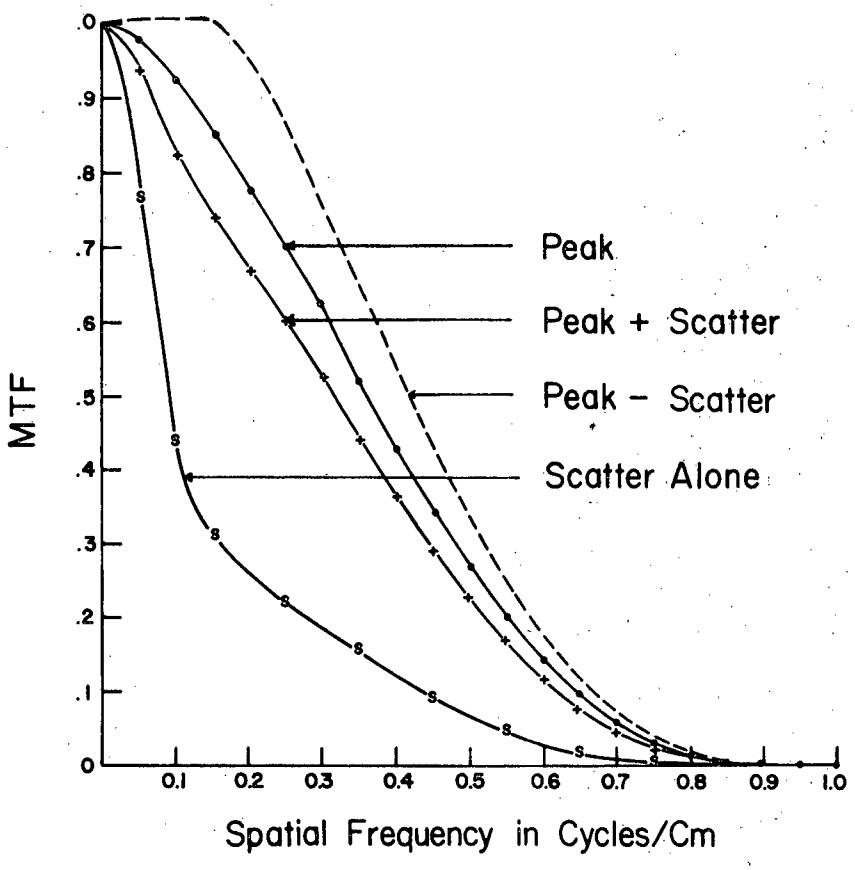

Figure 9. Modulation Transfer Functions for the response functions in Figures 6 and 7. Note that scatter subtraction yields uniformly highest MTF.

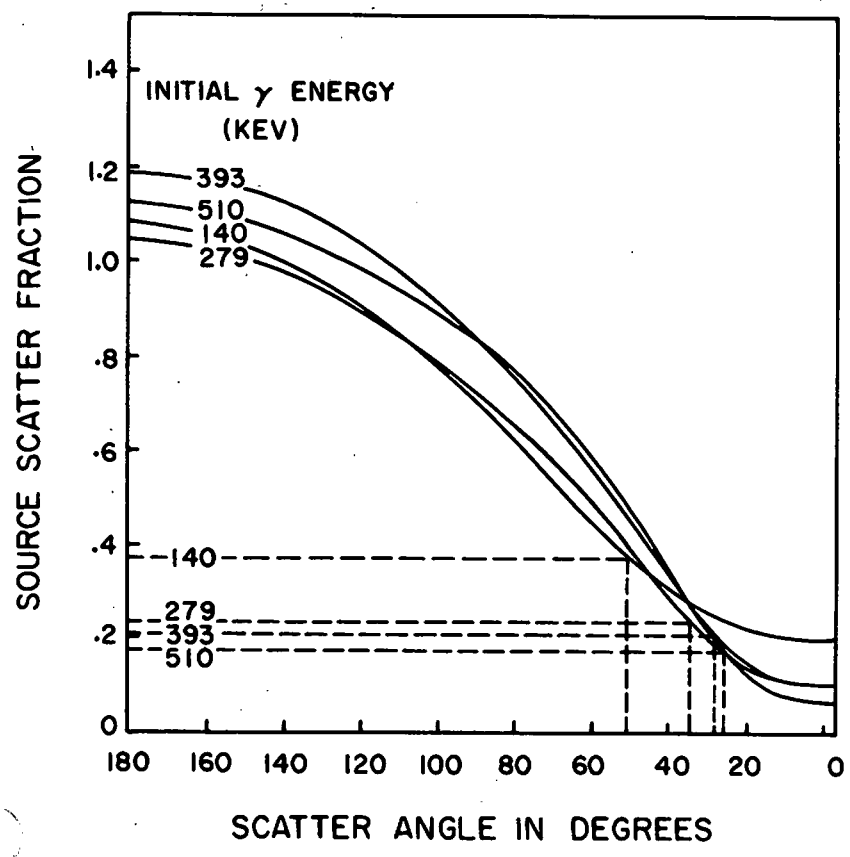
INITIAL γ ENERGY
(KEV)
393
510
140
279
1.4
1.2
1.0
.8
.6
.4
.2
0
140
279
393
510
180
160
140
120
100
80
60
40
20
0
SOURCE SCATTER FRACTION
SCATTER ANGLE IN DEGREES

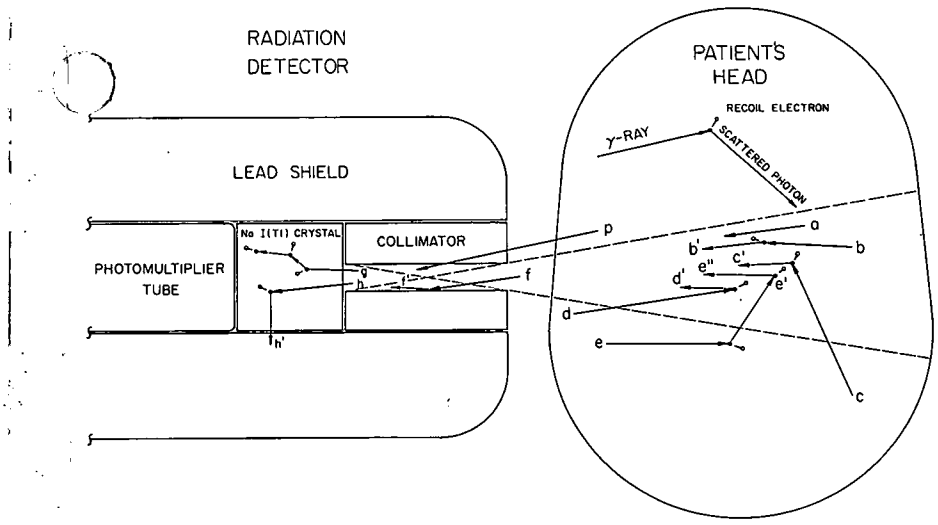
RADIATION
DETECTOR
LEAD SHIELD
PHOTOMULTIPLIER
TUBE
Na I(Tl) CRYSTAL
COLLIMATOR
PATIENT'S
HEAD
RECOIL ELECTRON
γ-RAY
SCATTERED PHOTON
p
a
b
b'
c'
d'
e''
e'
d
e
c
f
g
h
h'

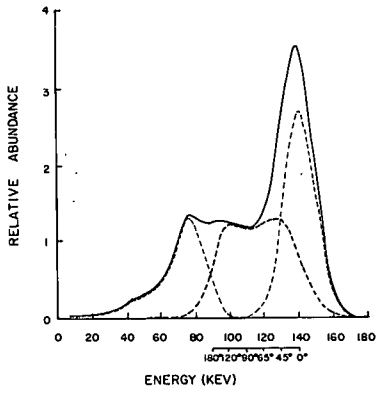
RELATIVE ABUNDANCE
0
1
2
3
4
0 20 40 60 80 100 120 140 160 180
180°120°90°65°45° 0°
ENERGY (KEV)

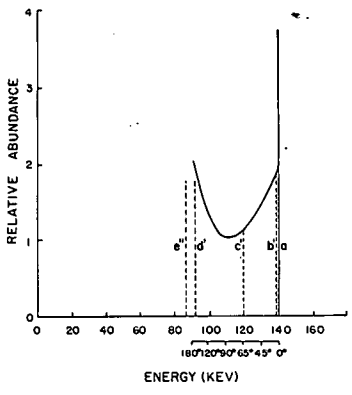
RELATIVE ABUNDANCE
0
1
2
3
4
e''
d'
c'
b'
a
0 20 40 60 80 100 120 140 160
180°120°90°65°45° 0°
ENERGY (KEV)

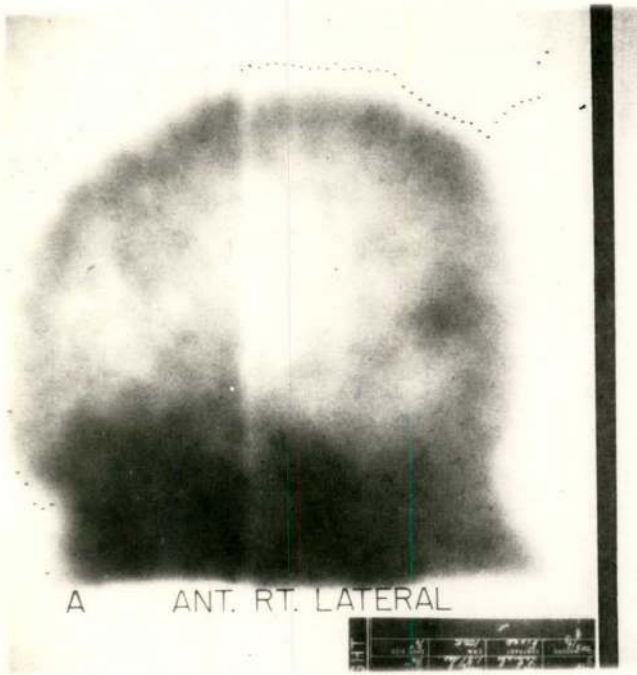

A ANT. RT. LATERAL

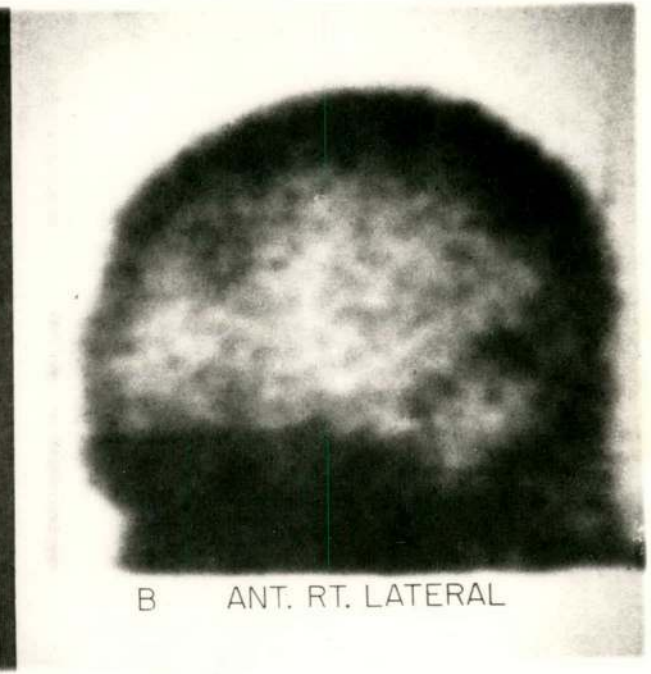

B ANT. RT. LATERAL

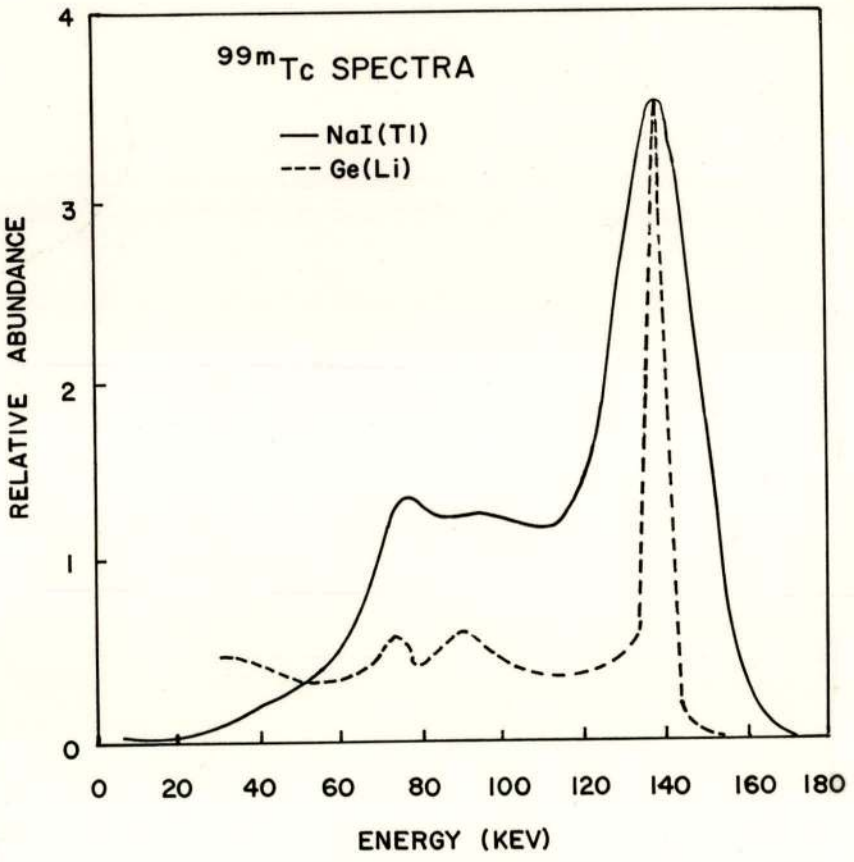
99m Tc SPECTRA
NaI(Tl)
Ge(Li)
RELATIVE ABUNDANCE
0
1
2
3
4
0
20
40
60
80
100
120
140
160
180
ENERGY (KEV)

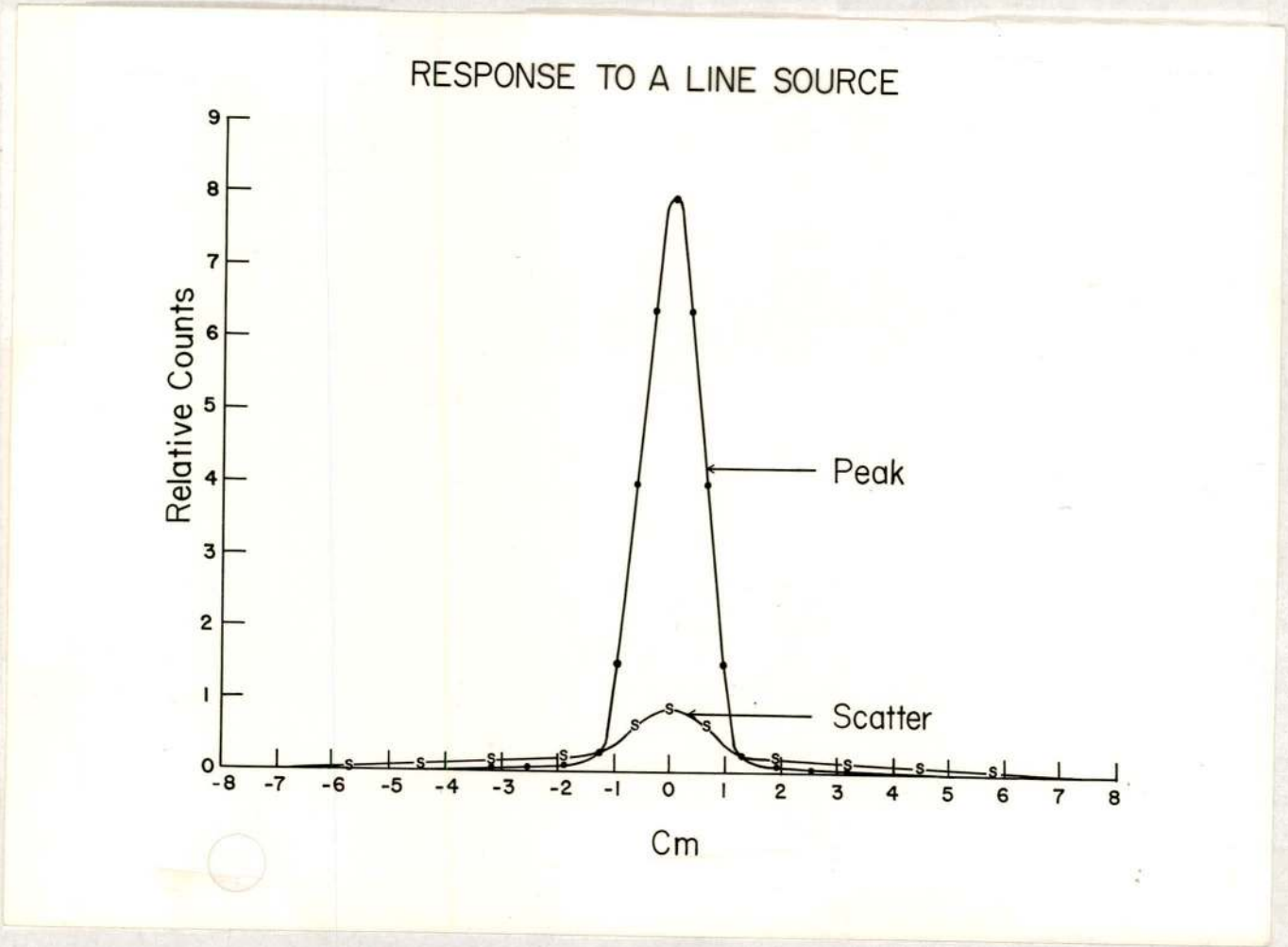
RESPONSE TO A LINE SOURCE
Relative Counts
0
1
2
3
4
5
6
7
8
9
-8 -7 -6 -5 -4 -3 -2 -1 0 1 2 3 4 5 6 7 8
Cm
Peak
Scatter

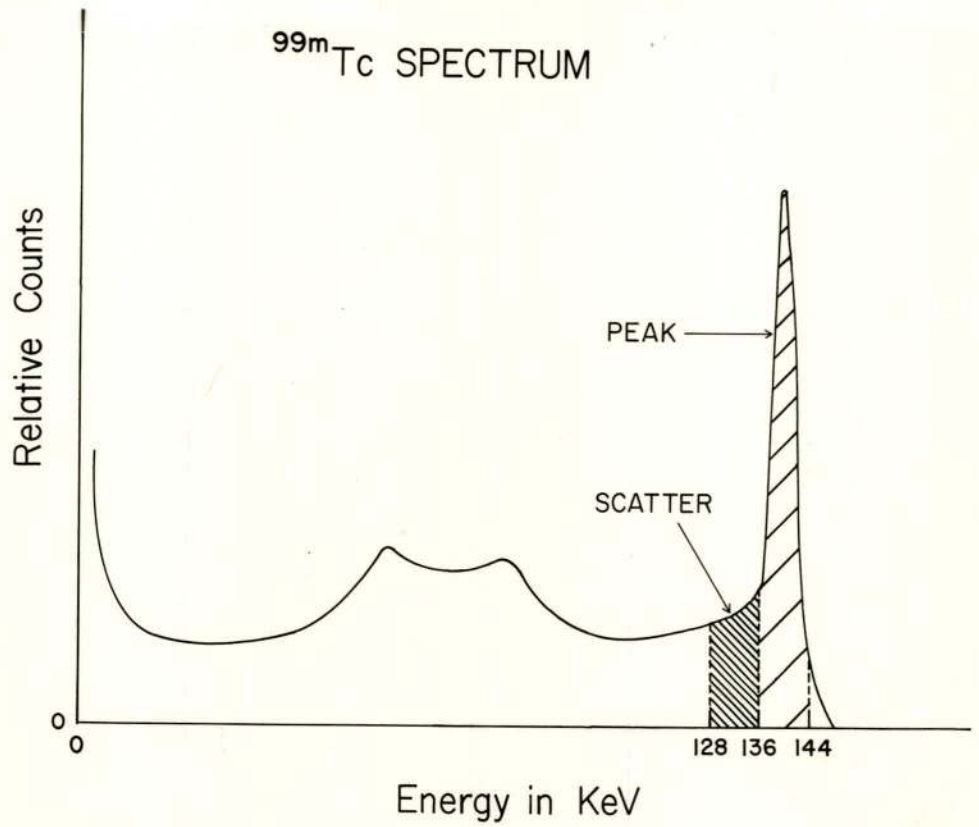
99m Tc SPECTRUM
Relative Counts
PEAK
SCATTER
0
0
128 136 144
Energy in KeV

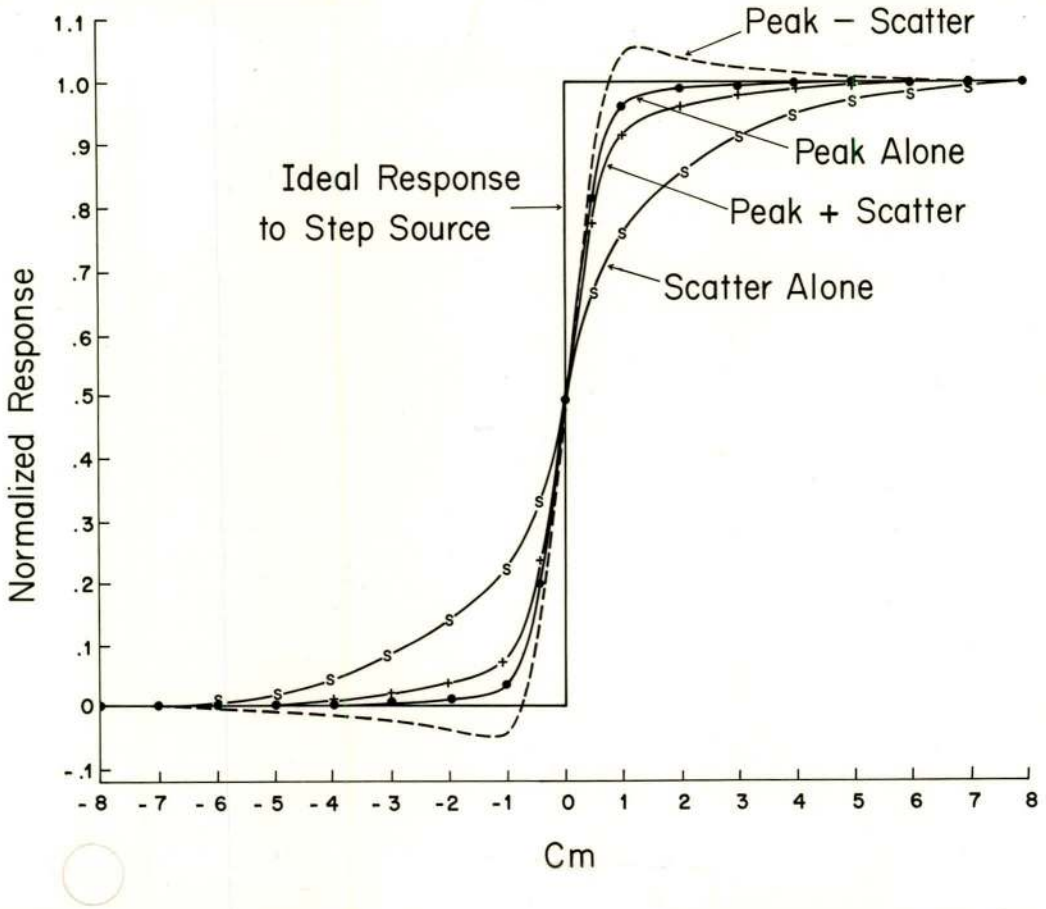
Peak − Scatter
Peak Alone
Peak + Scatter
Scatter Alone
Ideal Response
to Step Source
Normalized Response
1.1
1.0
.9
.8
.7
.6
.5
.4
.3
.2
.1
0
-.1
-8 -7 -6 -5 -4 -3 -2 -1 0 1 2 3 4 5 6 7 8
Cm

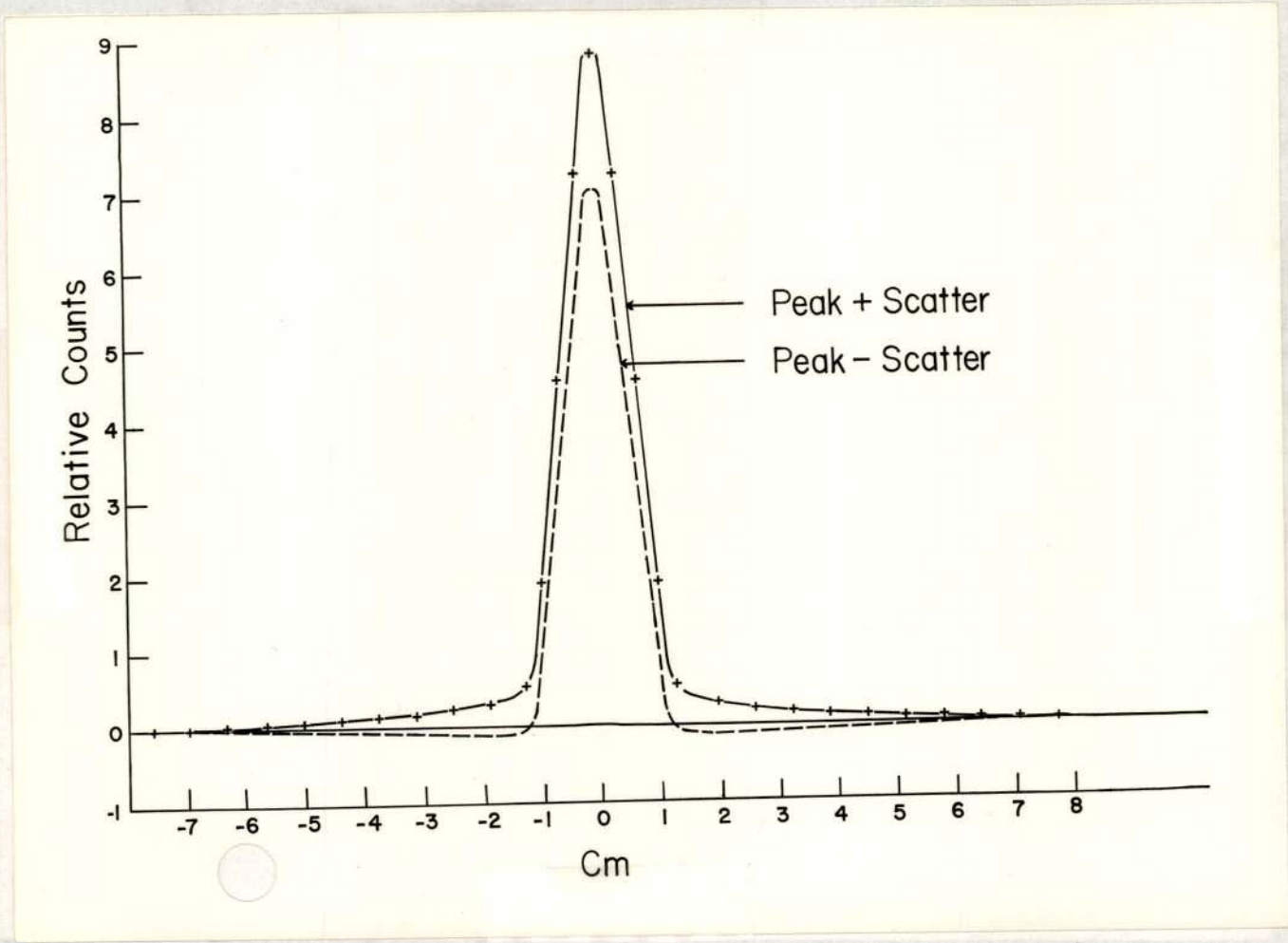
Relative Counts
9
8
7
6
5
4
3
2
1
0
-1
-7
-6
-5
-4
-3
-2
-1
0
1
2
3
4
5
6
7
8
Cm
Peak + Scatter
Peak – Scatter

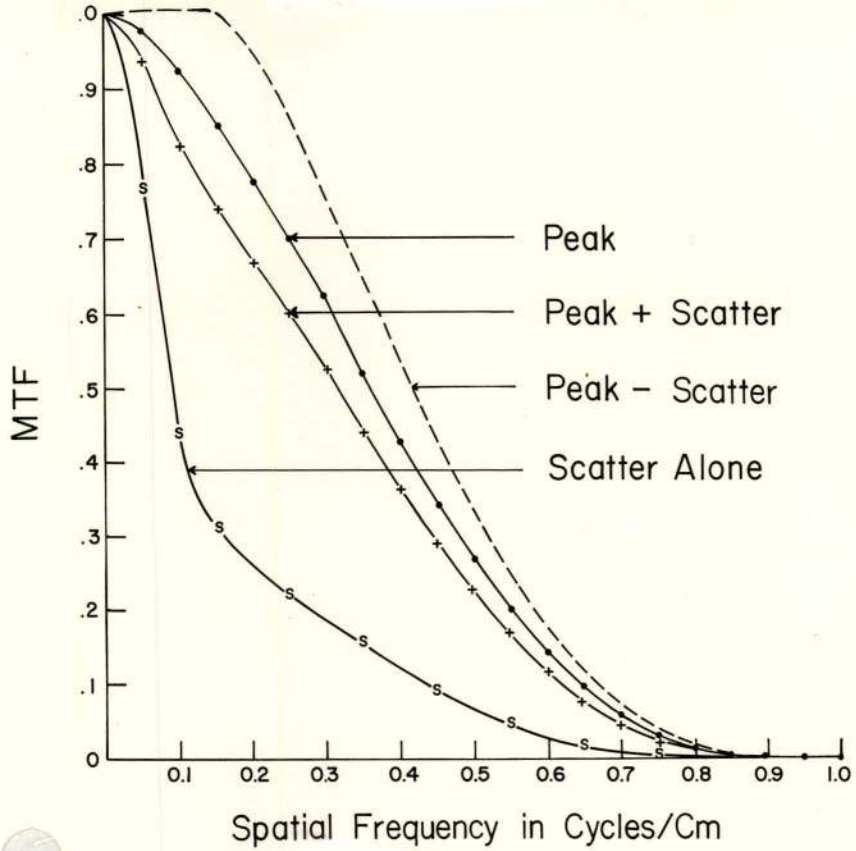
MTF
.0
.9
.8
.7
.6
.5
.4
.3
.2
.1
0
0.1
0.2
0.3
0.4
0.5
0.6
0.7
0.8
0.9
1.0
Peak
Peak + Scatter
Peak − Scatter
Scatter Alone
Spatial Frequency in Cycles/Cm